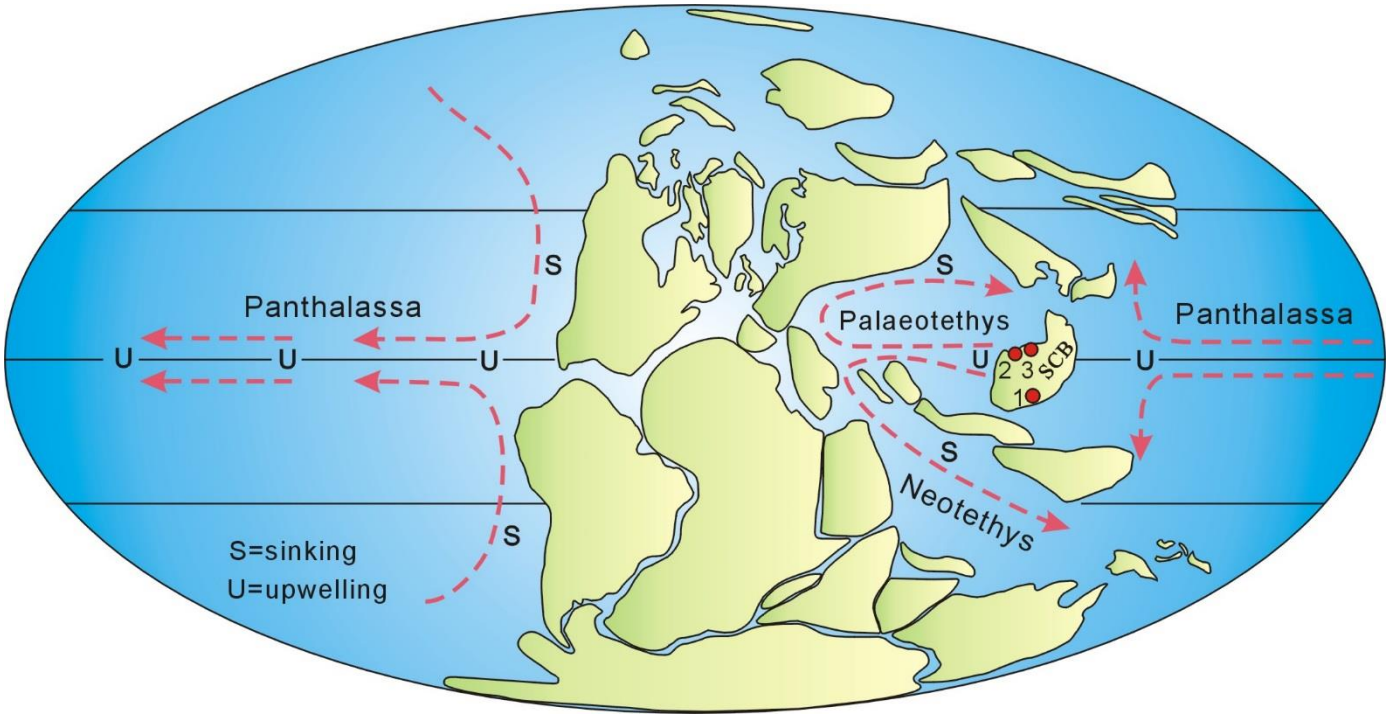

Fig. 1. Locations of the Dajiang section (1) in the south part of the South China Block (SCB) and the Laolongdong (2) and Cili (3) sections in the north part of the SCB. The earliest Triassic global palaeogeography map is modified from Golonka (2002).

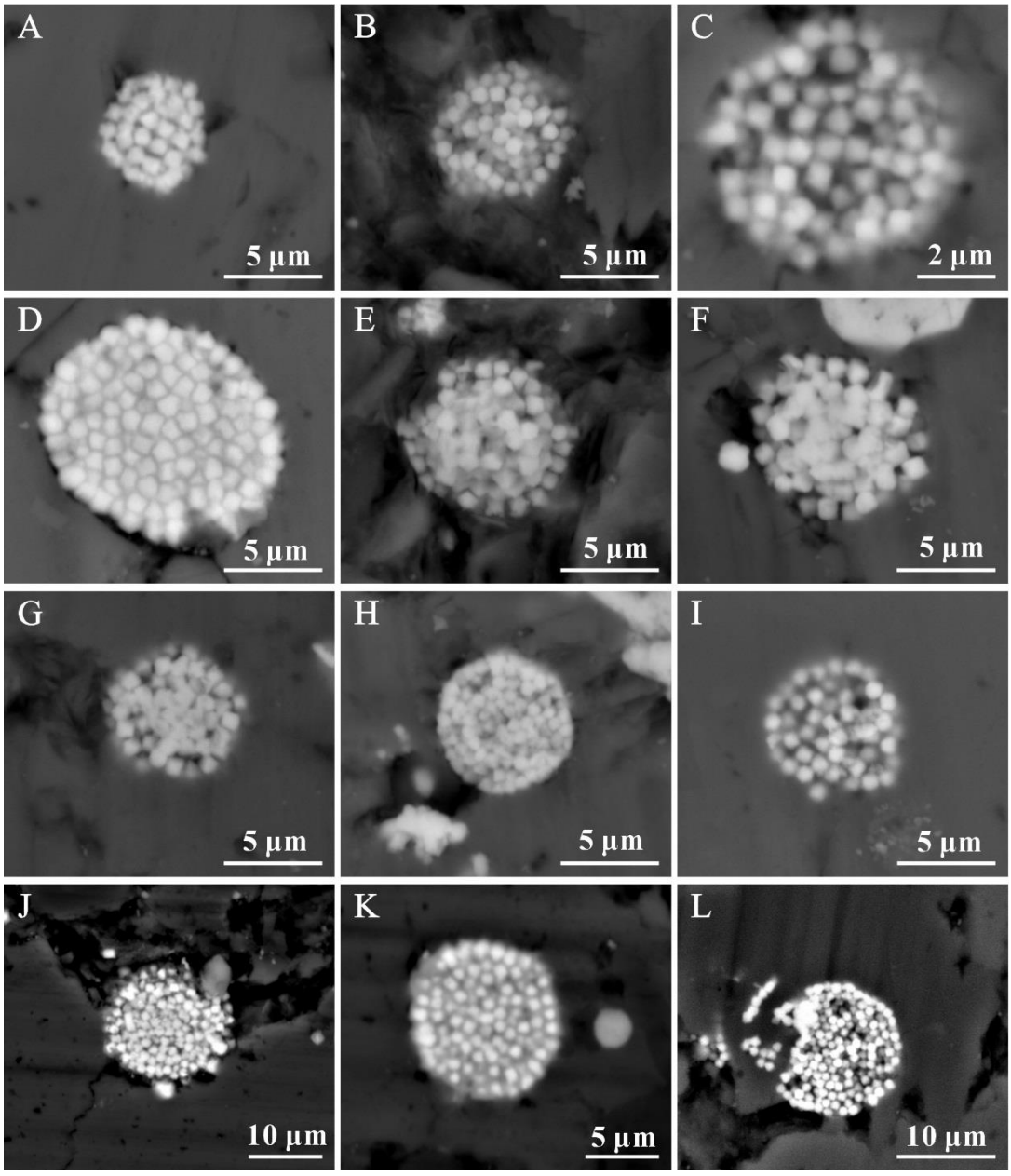

Fig. 2. Backscattered electron images of pyrite framboids in the Dajiang section.

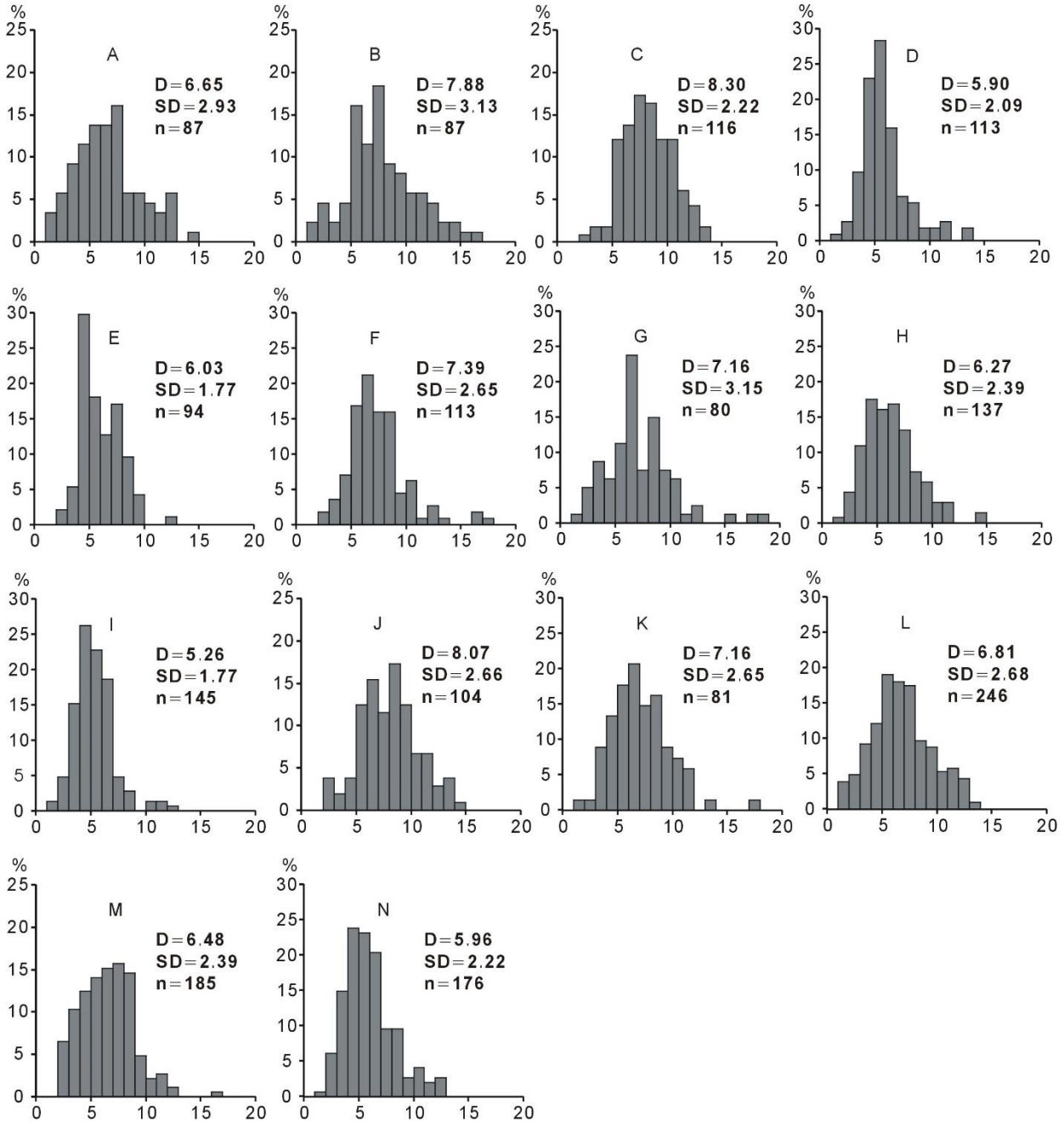

Fig. 3. Size distributions of the pyrite framboids in the Dajiang section. D = mean diameter of the framboids (μm); SD = standard deviation of the measurements; n = number of pyrite framboids measured in each sample. Each histogram corresponds to the samples marked from A to N in the section column of Fig. 4.

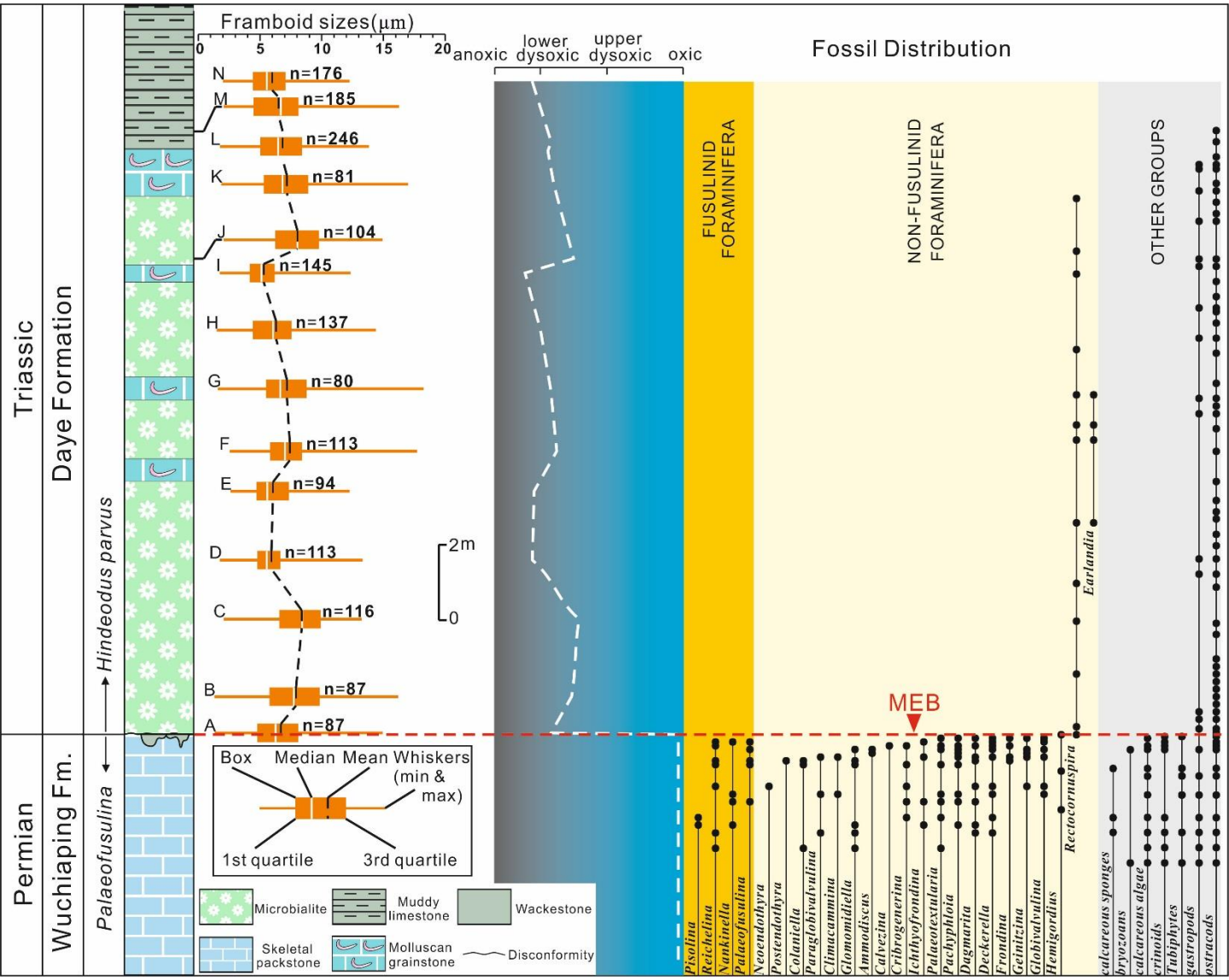

Fig. 4. “Box-and-whisker” plots of the diameters and the size range of pyrite framboids found in the Dajiang section, along with inferred water-column redox conditions and stratigraphic occurrences of fossils. The MEB coincides with an abrupt deficiency of oxygen content in bottom waters. Conodont and foraminifer data are from Jiang et al. (2014) and Song et al. (2009) respectively. Samples in the section column correspond to the histograms marked from A to N in Fig. 3.

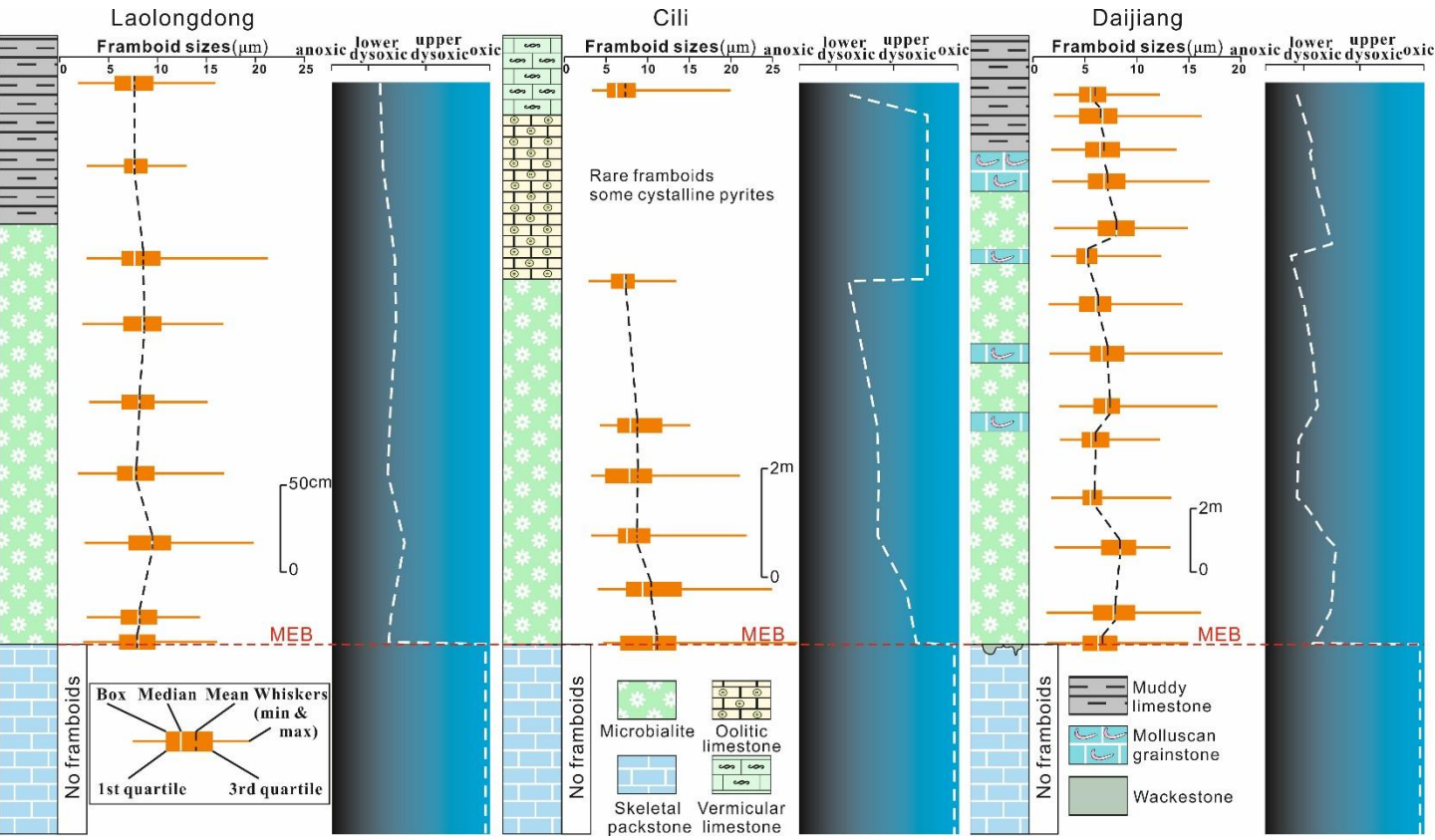

Fig. 5. Pyrite framboid "box-and-whisker" plots and inferred redox variations across the MEB in the shallow-marine carbonate platform of the SCB. The data of the Laolongdong section and the Cili section are from Liao et al. (2010) and He (2013) respectively.

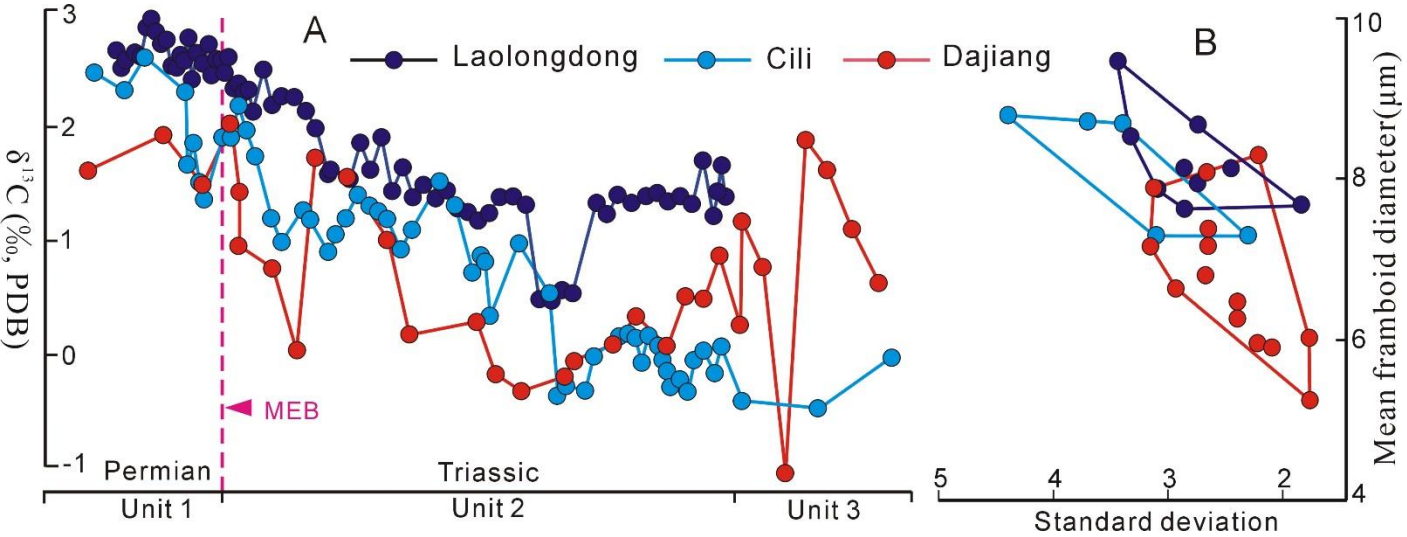

Fig. 6. $\delta^{13}C_{carb}$ (A) and pyrite framboid size (B) variations during Permian-Triassic transition in the shallow-marine carbonate platform of the SCB. Unit 1: the skeletal limestone below the MEB; Unit 2: the microbialite; Unit 3: the deposits above the microbialite. The $\delta^{13}C_{carb}$ data of the Laolongdong, Cili and Dajiang sections are from Liao et al. (2010), Luo et al. (2010) and Payne and Kump (2007), respectively. The pyrite framboid data of the Laolongdong and Cili sections are from Liao et al. (2010) and He (2013), respectively.